Inorganic Chemistry

Article

pubs.acs.org/IC

Metal Site-Mediated, Thermally Induced Structural Changes in Cr^{6+}-Silicalite-2 (MEL) Molecular Sieves

Yuchuan Tao,[†] Adrian Lita,[†] Lambertus J. van de Burgt,[†] Haidong Zhou,[‡] and A. E. Stiegman*[,†]

[†]Department of Chemistry and Biochemistry and [‡]National High Magnetic Field Laboratory, Florida State University, Tallahassee, Florida 32306, United States

ABSTRACT: Cr^{6+} ions were incorporated into the lattice sites of phase-pure silicalite-2 made using 3,5-dimethylpiperidinium as a structure-directing agent. The materials exhibited a remarkably well-resolved vibronic emission consisting of a high frequency progression of 987 cm^{-1}, which was assigned to the fundamental symmetric stretching mode of the $(Si-O-)_2Cr(=O)_2$ group dominated by the terminal Cr=O stretch. A low frequency progression at 214 cm^{-1}, which was assigned to a symmetric O−Cr−O bending mode, was built on each band of the 987 cm^{-1} progression. Studies of the vibronic structure of the emission spectrum as a function of temperature and Cr ion concentration reveal an abrupt change in the Franck−Condon factor of the emission at 20 K for samples with very low Cr concentrations (0.03 mol %). The change in the Franck−Condon factor is attributed to a temperature-induced structural change in the coordination sphere of the metal ion. This structural change was found to be accompanied by a concomitant structural change in the lattice structure of the silicalite-2. This structural change, as studied by temperature-dependent X-ray diffraction, did not involve a crystallographic phase change but an abrupt decrease in the unit cell volume, caused specifically by a decrease in the *c*-axis. This structural change was not observed in pure silicalite-2, indicating that it is not intrinsic to the silicalite lattice. Moreover, no similar structural change was observed at higher Cr loading (1 mol %). This suggests that the presence of the Cr ions and the changes in the coordination geometry they undergo at low temperature induced the observed contraction in the silicalite-2 lattice, in effect acting as a thermal switch that decreases the unit cell volume.

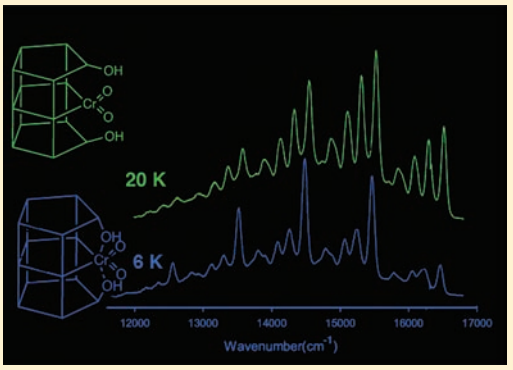

INTRODUCTION

In recent years there has been considerable interest in molecular-sieve materials containing redox active transition metals, which act as catalytic sites for performing oxidation reactions.[1] The paradigm for this class of materials is Ti-silicalite-1 (TS-1), which contains Ti^{4+} sites distributed in a silicalite-1 (ZSM-5) matrix.[2,3] This system was found to catalyze a number of oxidation reactions using hydrogen peroxide, including the oxidation of phenol to hydroquinone and the epoxidation of vinyl groups.[4] Early investigations aimed at characterizing TS-1 focused on determining the coordination environment of the titanium site, which proved to be a distorted tetrahedron from the isomorphic substitution of Ti^{4+} for Si^{4+} in the silicalite lattice. Considerable effort was also spent in determining whether the Ti substituted randomly in the available sites in the ZSM-11 structure or whether certain sites were preferentially occupied. The preponderance of data, obtained primarily from neutron-scattering studies, supports random occupation.[5−7] For TS-1 and other redox-active silicalite materials, the catalytic activity that is unique to these systems comes from a synergy between the silicalite lattice and the metal ions. In particular, the Lewis acidity of the metal site coupled with the hydrolytic lability of the Si−O−M linkages in the sieve give rise to hydrogen peroxide activation and subsequent oxidation of organic substrates in TS-1. Recently, we reported the synthesis and characterization of phase-pure, Cr-silicalite-2 (ZSM-11) redox-active sieve materials.[8] In this work, well-formed materials of high crystallographic quality containing up to 2.5 mol % Cr ions were synthesized. The Cr^{6+} site was incorporated into the silicalite lattice with retention of the C_{2v} terminal dioxo structure, $(SiO-)_2Cr(=O)_2$, which is well established for Cr^{6+} supported on amorphous silica.[9] As with other metal-substituted zeolites, we observed the expansion of the unit cell with the substitution of Cr^{6+} ions. In spectroscopic studies of these materials, we also observed an extremely unusual and previously unknown synergistic effect between a Cr and the overall crystal lattice. Specifically, we have found that Cr^{6+} ions, substituted at very low concentrations (0.03 mol %), undergo a thermally induced structural change in their coordination geometry that causes an abrupt contraction of the *c*-axis with a concomitant change in the unit cell volume. In effect, the structurally labile metal ion creates a thermal switch that can change the structural properties of the molecular sieve.

EXPERIMENTAL SECTION

Synthesis. Synthesis of Cr^{6+}-silicalite-2 was carried out using a previously published procedure.[8] Because of the dependence of the observed spectroscopic effects on the Cr concentrations, accurate

Received: November 7, 2011
Published: January 9, 2012

   dx.doi.org/10.1021/ic202401a | *Inorg. Chem.* 2012, 51, 2432−2437

determinations of the concentrations were carried out using ICP-MS. Specifically, samples for ICP-MS analyses were gravimetrically dissolved in 2% HNO_3 prepared using Optima grade HNO_3 and 18.3 MΩ MQ water under Class 100 clean lab conditions. The total dissolved solid (TDS) load of the samples was kept <2 ppm for efficient analyte ionization during ICP-MS analyses. Dissolved samples were analyzed by Agilent 7500cs quadrupole inductively coupled mass spectrometer (Q-ICP-MS) equipped with an octopole reaction cell (ORC). A precleaned quartz sample introduction system along with platinum extraction cones and a 100-μL nebulizer were used to minimize blanks. The Q-ICP-MS was operated under hot plasma conditions (1500W RF), and sensitivity was optimized prior to each set of analyses. The ORC cell was optimized to knock out plasma- and matrix-based interferences on analyte masses. External calibration using multielement ICP standard (high purity standard) coupled with indium (In) standard addition was performed for accurate concentration determination. The reproducibility for Cr, Mn, Fe, Co, Ni, and Zn on NIST SRM (1643e) was determined to be <3%.

Emission Spectroscopy. The emission spectra of Cr^{6+}-silicalite-2 were obtained using a 300 mm spectrograph (Acton Research Corporation Spectra Pro 308i, 150 g mm^{-1} grating blazed at 500 nm) and a back-thinned CCD (1340 × 400 pixels, Princeton Instrument LN/CCD-400EB-G1, operated at −90 °C). The sample was mounted in a Supertran-VP continuous flow (sample in vapor) cryostat (Janis Research Corporation). A Spectra-Physics DCR-3G Nd:YAG laser (10 Hz, 10 ns pulse, 1 J/pulse) operating in the third harmonic provided excitation at 355 nm. Emission excitation spectra were collected on a Spex Fluorolog II equipped with 0.22 m double monochromators (Spex 1680) and a 450 W Hg/Xe lamp. Front face (22.5°) collection was used to collect both emission and emission excitation spectra. Cutoff filters were used to suppress second-order excitation lines. Samples were mounted on an APD model DE-202 cryostat, shrouded, and evacuated. The samples were carefully aligned to maximize intensity in the detector prior to collection of spectra to ensure the best reproducibility of emission intensities. All reported spectra were corrected for the lamp profile and the detector response. Emission spectra reported in wavenumber units were corrected in the standard way for the bandpass variability in spectra collected at fixed wavelength resolution.[10]

Temperature-Dependent X-ray Diffraction. The X-ray powder diffraction (XRD) patterns were recorded by a HUBER imaging plate Guinier camera 670 with Cu Kα radiation (1.540 59 Å) with a Ge monochromator. Data were collected with temperatures down to 10 K obtained by a cryogenics compressor with He. Unit cell parameters were obtained through refinement of the strongest peaks in the diffraction pattern at each temperature in the tetragonal $I4\bar{m}2$ space group of ZSM-11.

RESULTS AND DISCUSSION

The series of d^0 metal ions (Ti^{4+}, V^{5+}, and Cr^{6+}) dispersed as isolated metal sites on amorphous silica all showed similar spectroscopic properties that consisted of long-lived luminescence arising from ligand-to-metal charge-transfer (LMCT) bands and resolved vibrational structure at frequencies characteristic of metal−oxygen modes coupled to the LMCT bands. The energy of the emission decreased across the series concomitant with the reduction potential of the ion. Due to the large amount of inhomogeneous broadening arising from the distribution of site geometries in the amorphous matrix, the emission spectra were typically quite broad, with the vibronic structure poorly resolved and appearing as a single mode between ∼950 and 980 cm^{-1} in the emission envelope. Chromium (6+) ions have been well studied spectroscopically, in part because they are the starting point for the generation of the Phillips ethylene polymerization catalyst.[11] The local coordination geometry of the Cr^{6+} sites is of C_{2v} symmetry, with two terminal oxo groups and two linkages to the silica network.[9,12] In an amorphous silica matrix, the Cr^{6+} site exhibits a long-lived (τ ∼30 μs) red luminescence, centered around 617 nm with a single resolved vibronic mode of ∼955 cm^{-1} in frequency.[9,13]

Our previous studies established that the C_{2v} coordination geometry is retained with substitution of Cr^{6+} in the silicalite-2 matrix.[8] Moreover, the materials that result are typically of excellent crystalline quality, a fact that is verified for the specific materials used in this study through XRD analysis and scanning electron microscopy.

Spectroscopically, the materials showed a red luminescence centered around 650 nm. The emission and excitation spectra, collected at 20 K, are shown in Figure 1. Apart from the average

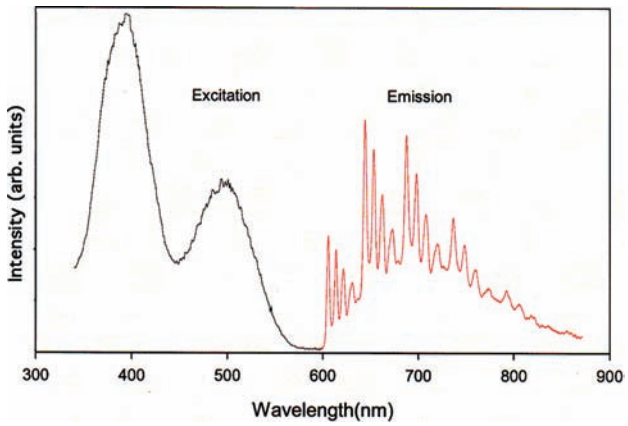

Figure 1. Emission (red) (355 nm excitation) and emission excitation spectra (644 nm monitor) collected at 20 K.

energy of the band, the spectrum differed dramatically from the emission observed for the Cr^{6+} site in amorphous silica.[9,13] Specifically, the spectrum exhibited an extremely well-resolved vibronic structure indicative of a relatively small amount of inhomogeneous broadening. The emission excitation spectrum, monitored at 644 nm, is also shown in Figure 1. The spectrum, consisting of two bands in the UV−vis region of the spectrum at 500 and 375 nm, was comparable to the diffuse reflectance electronic spectrum of Cr^{6+} in silicalite-2.[8] These observations are consistent with the origin of the structured emission being from the Cr^{6+} site and with the structure of the Cr^{6+} being similar across all types of silica support.[9] The Stokes shift between the emission maximum and the lowest energy band of the excitation spectrum was about 4600 cm^{-1}, which was anomalously large, suggesting that the excitation to the first excited state was likely a weak, spin-forbidden transition that was not observable in the spectrum. This is consistent with lifetime data, which show the excited state to be a long-lived phosphorescence. The broad emission spectra and poorly resolved vibrational structure of Cr^{6+} sites in amorphous silica are generally thought to arise from inhomogeneous broadening, due to the distribution of site symmetries that occur in the amorphous matrix. As such, the sharpness of the vibronic bands in Cr^{6+}-silicalite-2 likely arose from identical or nearly identical site symmetries imposed by the crystalline matrix, which reduced inhomogeneous broadening.

While no vibronic structure was observed in the excitation spectrum, the first resolved mode of the first progression of the emission spectrum overlaps the red edge of the excitation spectrum and is assigned as E_{00} at 16 505 cm^{-1}. Detailed analysis of the resolved vibronic modes indicated that they are

dx.doi.org/10.1021/ic202401a | *Inorg. Chem.* 2012, 51, 2432−2437

composed of a long progression at ~987 cm^{-1}, of which the $\nu(0-0)$ though $\nu(0-4)$ modes are well resolved, with the most intense transition being the $\nu(0-1)$ mode (black ladder diagram, Figure 2). A low frequency mode of ~214 cm^{-1} was

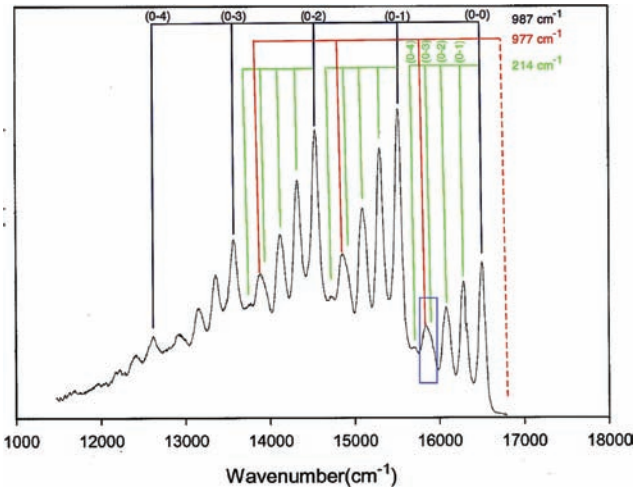

Figure 2. Emission spectrum of 0.03 mol % Cr-silicalite-2 collected at 20 K with 355 nm excitation.

built on each of the high frequency modes (green ladder diagram, Figure 2). The 985 cm^{-1} was well characterized and was assigned to a symmetric stretch of the $(Si-O)_2Cr(=O)_2$ moiety dominated by the terminal oxo bonds.[9,14−17] The low frequency mode has not been assigned spectroscopically; however, reliable calculations by Dines and Inglis predict a relatively intense, totally symmetric low-frequency mode at 214 cm^{-1}, which is composed of primarily O−Cr−O bending, which is a reasonable assignment.[14] Close inspection of the peak shapes of the vibronic modes revealed that the bands associated with every fourth mode $\nu(0-3)$ of the short progression showed evidence of two overlapping bands, as can be seen in the blue box in Figure 2. In fact, on the basis of the frequency of the short modes, the position of the $\nu(0-3)$ band fell on the shoulder of the band, suggesting that another mode was present. This mode appeared to be another long mode of ~980 cm^{-1}, associated with the chromium dioxo symmetric stretch, which starts from a different origin than the other resolved modes. The origin could begin at 15 878 cm^{-1} where the first band was observed or, possibly, at 16 855 cm^{-1} (dashed red line in Figure 2). A band at the latter position was not directly seen in the spectra, but it simply may be too weak to observe.

The vibrational structure in the emission spectra of the Cr site was carried out using the time-dependent theory, initially developed by Heller and utilizing equations provided by Zink.[18−23] The spectral simulations generated by this method rely on several key parameters, including the frequencies of the resolved vibronic modes, the normal coordinate change, Δ, which in the time-dependent simulations is a unitless parameter, and the damping factor, Γ, which accounts for both homogeneous and inhomogeneous components of spectral broadening. In addition, to simulate the full width of the spectrum, additional modes, unresolved in the spectrum but known to be present in the molecule, were added to improve the simulation.

The emission spectrum collected at 20 K and its simulation are shown in Figure 3a. An excellent simulation was obtained

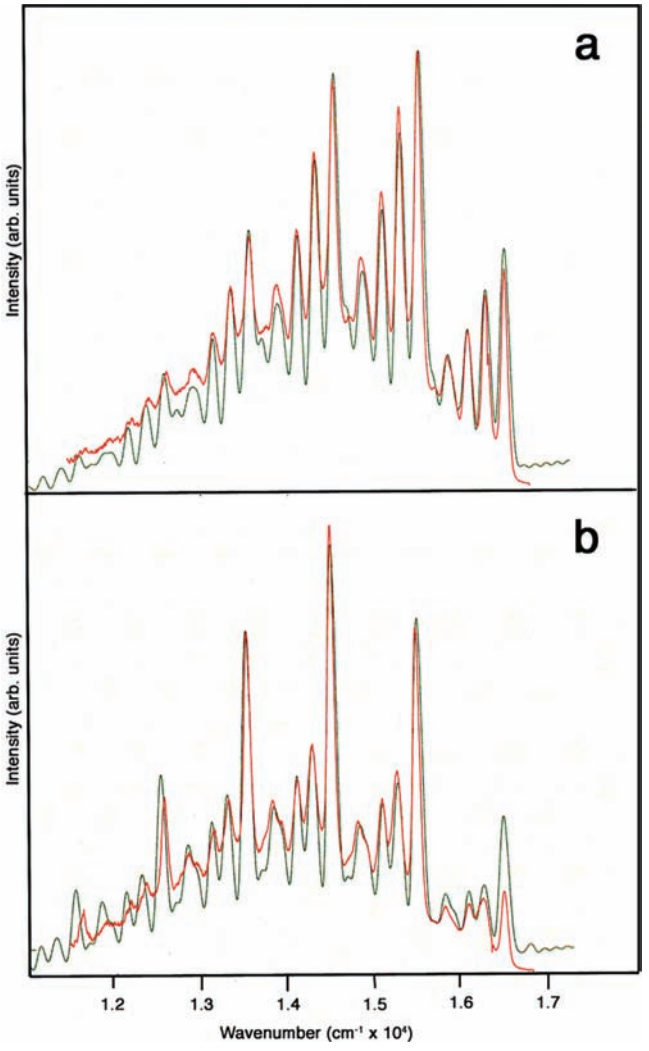

Figure 3. Emission spectrum (red) and emission simulation (green) of 0.03 mol % Cr-silicalite-2 excited at 355 nm collected at (a) 20 K and (b) 6 K.

using the high-frequency 986 cm^{-1} mode associated with the $(Si-O)_2Cr(=O)_2$ symmetric stretch, upon which a low frequency mode at 214 cm^{-1} was built (Table 1, shaded in gray). To fully simulate the spectral envelope, which was composed of unresolved modes of the $(Si-O)_2Cr(=O)_2$ group, additional modes were added (Table 1, unshaded), all of which were taken from the calculations of Dines and Inglis for the $(Si-O)_2Cr(=O)_2$ species.[14] This resulted in a very good simulation of the spectra. The normal coordinate change for each mode used and the damping factor used to achieve the best simulation are given in Table 1. Interestingly, the additional long mode discussed above was also included, which improved the agreement between the simulation and the spectra significantly. The values for the frequency and displacement of this mode that yielded an optimum simulation proved very close to the primary long mode $(Si-O)_2Cr(=O)_2$ symmetric stretch (977 and 987 cm^{-1}, Δ = 2.20 and 2.02, respectively; Table 1), suggesting that this progression, which has a completely different origin, is likely a $(SiO)_2CrO_2$ symmetric stretch emanating from a Cr sitting in another

dx.doi.org/10.1021/ic202401a | Inorg. Chem. 2012, 51, 2432−2437

Table 1. Frequencies and Parameters Used in Time-Dependent Simulations

Frequency (cm^{-1})	Δ	Γ (cm^{-1})
20 K		
987	2.02	38
214	1.32	
423	0.80	
587	0.70	
798	0.58	
977	2.20	10
6 K		
1001	2.35	38
240	1.05	
404	0.90	
596	0.70	
778	0.55	
991	2.90	10

distinct crystallographic site in the lattice. The low intensity of the modes suggested that it was either an inherently weak emission or the site was more poorly populated.

Upon cooling of the sample from room temperature to 20 K, the emission spectrum underwent the expected intensity increase and band sharpening, but the positions of the vibrational bands remained unchanged. In the temperature range between 20 and 9 K, however, there was an abrupt change in the emission band shape and a shift in the centroid of the emission toward lower energy. The shift in band position was accompanied by a systematic change in the intensity distribution of vibronic modes, in that there was an increase in intensity of the vibrational progression going to lower energy so that, for example, below 20 K the $\nu(0-2)$ modes became as intense as the $\nu(0-1)$ mode. Changes in the emission band shape and the intensity distribution of the resolved vibronic modes are directly governed by the normal coordinate change between the ground and excited state.

The magnitude of the normal coordinate change, Δ, could also be determined by calculating the Huang–Rhys factor from the spectral data, which provided a convenient method of correlating the structural change with the temperature. The Huang–Rhys factor, S, for the vibronic mode, n, was determined from the ratio of the intensities of the $\nu(0-0)$ and $\nu(0-n)$ modes (eq 1a).[24] In this work, the Huang–Rhys factor was determined from the ratio of the intensity of the $\nu(0-0)$ and $\nu(0-1)$ transitions of the high frequency mode, which is related to the normal coordinate change, Δ, between the ground and excited state through eq 1b.

$$I_n = \frac{S^n}{n!} I_0 \tag{1a}$$

$$S^1 = \frac{I_{(0,1)}}{I_{(0,0)}} = \frac{\Delta}{\sqrt{2}} e^{-\Delta^2/4} \tag{1b}$$

For Cr^{6+}-silicalite-2, a plot of S as a function of temperature is shown in Figure 4. As can be seen, at temperatures above 20 K,

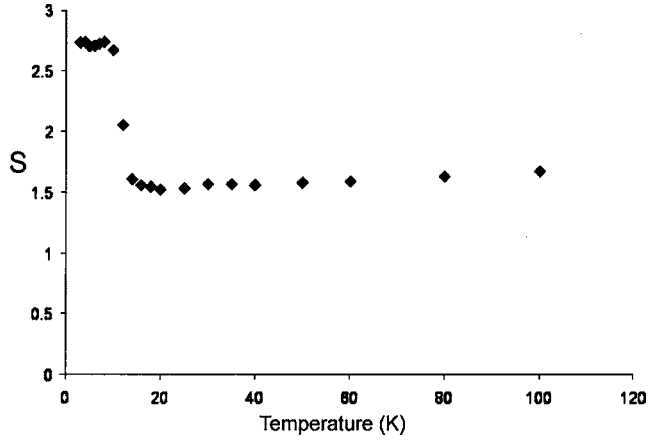

Figure 4. Dependence of the Huang–Rhys factor (S) calculated from the vibronic progression in the emission spectra of 0.03 mol % Cr-silicalite-2 as a function of temperature.

S decreased slightly with temperature, reaching a value of ~1.5 at 20 K. Below 20 K, there was a very abrupt change in the magnitude of S, which almost doubles and then plateaus at a maximum of 2.75 at 10 K. A change such as this must be due to a relatively abrupt structural change around the chromium site in the crystal lattice as the temperature drops below 20 K. While the abrupt change in the Huang–Rhys factor was evidence of a change in the structure of the Cr site, the primary characteristics of the resolved vibronic bands in the emission, in particular the high frequency symmetric stretch with the low-frequency progression built on it, were still present, which suggests that what occurred was not a drastic change in the geometry of the molecule to a different point group but instead a more modest rearrangement of the coordination sphere. Ideally, direct measurement of the vibrational spectra of the Cr site might provide information about the structural change, but unfortunately, the low concentration at which the Cr was present precluded this. In an attempt to extract some information from the resolved vibronic modes in the emission spectra, further simulations using the time-dependent theory were carried out on the emission spectrum collected at 6 K. This was done by adjusting the frequency, displacement, and damping factors of the existing set of frequencies to bring them into agreement with the 6 K spectrum. As can be seen in Figure 3b, a reasonably good simulation was obtained by means of this approach using the parameters listed in Table 1. As would be expected from the change in Huang–Rhys factors, the normal coordinate change required to achieve a good simulation increased in value. More importantly, to achieve a good simulation, higher frequencies of the observed modes were required. While it is not possible to come up with any details of the structural change, the fact that the same modes appeared to be still present after the thermal transition, albeit at somewhat higher frequencies, indicated that the primary metal–oxygen bonds comprising the $(Si-O)_2Cr(=O)_2$ site were still intact. From the standpoint of vibrational modes, one structural interaction that would be expected to increase the vibrational frequencies while retaining the same molecular structure would be enhanced bonding into the silicalite network. As discussed in our previous study, the placement of the $(Si-O)_2Cr(=O)_2$ site

dx.doi.org/10.1021/ic202401a | Inorg. Chem. 2012, 51, 2432–2437

in the silicalite matrix imposes steric strain because of the large size of the CrO_2 unit and the fact that it occupies a tetrahedral site in the lattice through only two bonds, leaving, presumably, two dangling Si−OH groups in close proximity to the Cr. This is directly manifested in the large unit cell volume change (for a small Cr^{6+} ion) of the silicalite lattice as a function of Cr concentration. As the temperature decreases, the unit cell dimensions contract, consistent with conventional thermal expansion parameters. At a certain point, corresponding in our system to ∼20 K, the proximity of the dangling Si−OH groups and the Cr center is close enough for bonding interactions to occur. The addition of electron density from the lone pairs on the oxygen to the empty d orbitals on the high-valent (i.e., electron deficient) Cr ion provides the driving force for bond formation. When this happens, coupling of the $(Si-O)_2Cr(=O)_2$ unit to the lattice becomes stronger (i.e., additional Si−O−Cr force constants contribute to the normal mode), leading to higher frequencies of the existing modes. This postulated process is shown schematically in Figure 5.

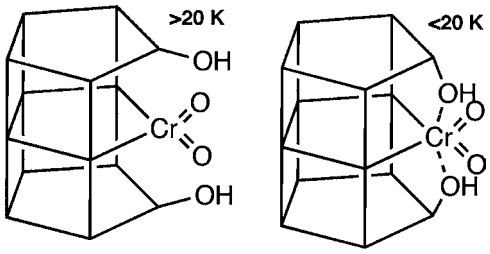

Figure 5. Schematic showing the proposed origin of the abrupt structural changes due to dative bond formation of the between dangling silanols and the Cr^{6+} ions.

If this hypothesis is correct, we would expect there to be an abrupt contraction of the silicalite in the region of the coordination sphere of the Cr ion. This contraction should be accompanied by a change in the unit cell dimensions of the silicalite matrix. To test this hypothesis, powder X-ray diffraction (XRD) data of the Cr^{6+}-silicalite-2 materials were collected as a function of temperature. The results of this study are shown in Figure 6. For pure silicalite-2 (0% Cr), there is a relatively monotonic decrease in the lattice dimensions and the unit cell volume as a function of temperature associated with conventional thermal contraction. The decrease begins to plateau below ∼40 K, and no unusual behavior is observed below 20 K. For the 0.03 mol % sample, however, the monotonic contraction in the unit cell parameters parallel the pure silicalite-2 until ∼20 K, where the spectroscopic changes are observed in the Cr emission. At that temperature an abrupt drop in the unit cell volume occurs. Interestingly, the abrupt contraction in the unit cell volume is caused by a sharp decrease in the length of the *c*-axis, but not by changes in the *a*-, *b*-axes which have ceased to change significantly by ∼30 K. This is consistent with the Cr ions, at very low loading, not being randomly distributed but instead preferentially occupying a specific site or limited distribution of sites in the lattice. The specific location of the sites being such that thermally induced changes in the coordination geometry of the Cr will result in a contraction of the lattice along a specific crystallographic direction. As noted previously, this structural change is not observed at concentrations of 0.5 mol % and greater. While the vibrationally structured emission is observed at higher loadings, there is no abrupt change in the Huang−Rhys factor when the

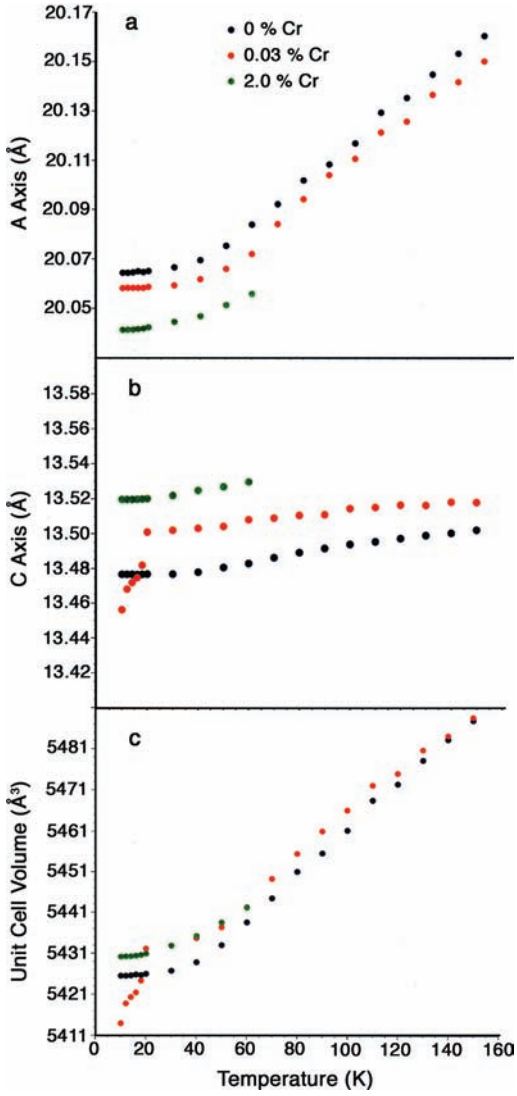

Figure 6. Change in the unit cell of the (a) *a*-axis, (b) *c*-axis, and (c) volume of 0, 0.03, and 2.0 mol % Cr-silicalite-2 as a function of temperature.

temperature dropped below 20 K. For a 2.0 mol % sample, temperature-dependent XRD (Figure 6) confirmed that no abrupt changes in the lattice parameters were observed at 20 K or below. A plausible explanation for this is that higher Cr loadings expand the lattice parameters so that even with the contraction that occurs during cooling the close proximity interactions between the silanols and the Cr is not attained so that bonding interactions cannot form. While this explanation appears plausible we cannot rule out other processes that may be occurring and that may also explain the phenomenon.

In summary, we have observed that small amounts of Cr ions incorporated into a silicalite-2 lattice can induce structural changes as a function of temperature: a phenomenon that we do not believe has been previously reported. We were able to observe this both through the changes in the immediate coordination environment around the metal atoms and through the concomitant structural changes in the silicalite crystal lattice as a whole. We observed the former through the temperature-dependent changes in the vibronic structure of the emission and the latter through the changes in the crystallographic parameters that occur at the same temperature. Our

dx.doi.org/10.1021/ic202401a | *Inorg. Chem.* 2012, 51, 2432−2437

observation of metal site-induced structural changes in a molecular sieve material affords, possibly, a strategy for building thermomechanical or thermo-optical properties into such sieve materials by the incorporation of structurally labile metal sites.

AUTHOR INFORMATION

Corresponding Author
*E-mail: stiegman@chem.fsu.edu.

ACKNOWLEDGMENTS

We thank Dr. Nicole Tibbetts, Dr. Sambuddha Misra, and Dr. Afi Sachi-Locher of the Department of Geochemistry, National High Magnetic Field Laboratory, for performing Cr analysis on our samples. This work was funded under the auspices of the National Science Foundation under Grant CHM-0911080.

REFERENCES

(1) Arends, I. W. C. E.; Sheldon, R. A.; Wallau, M.; Schuchardt, U. *Angew. Chem., Int. Ed. Engl.* **1997**, *36*, 1145.
(2) Notari, B. *Catal. Today* **1993**, *18*, 163.
(3) Notari, B. *Adv. Catal.* **1996**, *41*, 253.
(4) Smith, G. V.; Notheisz, F. *Heterogeneous Catalysis in Organic Chemistry*; Academic Press: San Diego, 1999.
(5) Henry, P. F.; Weller, M. T.; Wilson, C. C. *J. Phys. Chem. B* **2001**, *105*, 7452.
(6) Hijar, C. A.; Jacubinas, R. M.; Eckert, J.; Henson, N. J.; Hay, P. J.; Ott, K. C. *J. Phys. Chem. B* **2000**, *104*, 12157.
(7) Lamberti, C.; Bordiga, S.; Zecchina, A.; Artioli, G.; Marra, G.; Spano, G. *J. Am. Chem. Soc.* **2001**, *123*, 2204.
(8) Lita, A.; Tao, Y.; Ma, X. S.; van de Burgt, L. J.; Stiegman, A. E. *Inorg. Chem.* **2011**, *50*, 11184.
(9) Moisii, C.; Deguns, E. W.; Lita, A.; Callahan, S. D.; van de Burgt, L. J.; Magana, D.; Stiegman, A. E. *Chem. Mater.* **2006**, *18*, 3965.
(10) Lakowicz, J. R. *Principles of Fluorescence Spectroscopy*; Plenum: New York, 1983.
(11) Groppo, E.; Lamberti, C.; Bordiga, S.; Spoto, G.; Zecchina, A. *Chem. Rev.* **2005**, *105*, 115.
(12) Weckhuysen, B. M.; Wachs, I. E.; Schoonheydt, R. A. *Chem. Rev.* **1996**, *96*, 3327.
(13) Hazenkamp, M. F.; Blasse, G. *J. Phys. Chem.* **1992**, *96*, 3442.
(14) Dines, T. J.; Inglis, S. *Phys. Chem. Chem. Phys.* **2003**, *5*, 1320.
(15) Hardcastle, F. D.; Wachs, I. E. *J. Mol. Catal.* **1988**, *46*, 173.
(16) Vuurman, M. A.; Wachs, I. E.; Stufkens, D. J.; Oskam, A. *J. Mol. Catal.* **1993**, *80*, 209.
(17) Weckhuysen, B. M.; Wachs, I. E. *J. Phys. Chem. B* **1997**, *101*, 2793.
(18) Heller, E. J. *Acc. Chem. Res.* **1981**, *14*, 368.
(19) Acosta, A.; Zink, J. I. *J. Organomet. Chem.* **1998**, *554*, 87.
(20) Hanna, S. D.; Zink, J. I. *Inorg. Chem.* **1996**, *35*, 297.
(21) Preston, D. M.; Shin, K. S.; Hollingsworth, G.; Zink, J. I. *J. Mol. Struct.* **1988**, *173*, 185.
(22) Wexler, D.; Zink, J. I. *Inorg. Chem.* **1995**, *34*, 1500.
(23) Wexler, D.; Zink, J. I.; Reber, C. *J. Phys. Chem.* **1992**, *96*, 8757.
(24) Brunold, T. C.; Gudel, H. U. In *Inorganic Electronic Structure and Spectroscopy*, 1st ed.; Solomon, E. I., Lever, A. B. P., Eds.; Wiley: New York, 1999; Vol. *1*, p 259.